Supporting information for

Global metabolic reprogramming of colorectal cancer occurs at adenoma stage and is induced by MYC

Kiyotoshi Satoh, Shinichi Yachida, Masahiro Sugimoto, Minoru Oshima, Toshitaka Nakagawa, Shintaro Akamoto, Sho Tabata, Kaori Saitoh, Keiko Kato, Saya Sato, Kaori Igarashi, Yumi Aizawa, Rie Kajino-Sakamoto, Yasushi Kojima, Teruaki Fujishita, Ayame Enomoto, Akiyoshi Hirayama, Takamasa Ishikawa, M. Mark Taketo, Yoshio Kushida, Reiji Haba, Keiichi Okano, Masaru Tomita, Yasuyuki Suzuki, Shinji Fukuda, Masahiro Aoki, Tomoyoshi Soga*

correspondence to: Tomoyoshi Soga, E-mail: soga@sfc.keio.ac.jp

This PDF file includes:

SI Materials and Methods

Mouse strains

Construction of an *Apc*$^{+/\Delta 716}$ strain has been described previously (1). The strain was backcrossed to the C57BL/6N background for >20 generations. C57BL/6N mice were purchased from CLEA Japan (Tokyo, Japan). Mice were kept under a 12-hour light-dark cycle at ~22°C and fed ad libitum with a CLEA CE-2 chow diet. All animal experiments were conducted according to protocols approved by the Animal Care and Use Committee of the Aichi Cancer Center Research Institute.

Mouse tissue sample preparation

For metabolome analyses, intestinal polyps and normal intestinal tissue was excised from euthanized female mice, washed in ice-cold 5% w/v mannitol solution, snap-frozen in liquid nitrogen, and stored at -80°C. For RNA isolation, the intestinal tissue samples were washed in PBS and pretreated with RNAlater solution (Life Technologies, Carlsbad, CA) at 4°C overnight and then stored at -80°C.

Total RNA isolation from mouse tissue

Total RNA from mouse tissue was isolated using an RNeasy Mini Kit (Qiagen, Venlo, Netherlands) according to the manufacturer's protocol, including on-column DNase I incubation for 15 min at room temperature to reduce genomic DNA contamination.

Cell culture

The human colorectal carcinoma cell lines HCT116 and RKO and the human normal colorectal cell line CCD841 CoN were obtained from the American Type Culture Collection (ATCC). The human rectal adenocarcinoma cell line CaR-1 and human colorectal carcinoma cell line COLO741 were obtained from the Japanese Collection of Research Bioresources (JCRB) and the European Collection of Authenticated Cell Cultures (ECACC), respectively. The cells were maintained in Dulbecco's Modified Eagle's Medium (Sigma-Aldrich, St. Louis, MO) supplemented with 10% fetal bovine serum (Equitech-Bio, Kerrville, TX) at 37°C with 5% CO_2. For qRT-PCR, DNA microarray, and metabolome analyses, 2×10^5 cells were seeded in a 60-mm dish, cultured for 24 h, and transfected with 100 nM ON-TARGETplus siRNAs (Dharmacon, Lafayette, CO) using Lipofectamine RNAiMAX (Invitrogen, Carlsbad, CA) according to the manufacturer's instructions. For the cell proliferation assay, 5×10^4 cells were seeded in 60-mm dishes, cultured for 24 h, and transfected with 100 nM siRNAs. Three days after transfection, the cells were counted using a Cytell Cell Imaging System (GE Healthcare, Buckinghamshire, United Kingdom), following the manufacturer's instructions. The siRNA oligonucleotide sequences are listed in table S4.

Metabolite extraction from CRC and mouse tissue

The excised tissues were cut into pieces smaller than 1 cm^3, immediately frozen in liquid nitrogen, and stored at −80°C until metabolite extraction. To extract charged metabolites and glucose, pre-weighed, deep-frozen samples (approximately 50 mg each) were completely homogenized using a cell disrupter (Shake Master NEO; Bio Medical Science, Tokyo, Japan) at 1500 rpm for 5 min after the addition of 500 µL of methanol containing internal standards [20 µM each of methionine sulfone, 2-(N-morpholino)-

ethanesulfonic acid (MES) and D-camphor-10-sulfonic acid (CSA)]. The homogenate was then mixed with Milli-Q water and chloroform in a volume ratio of 5:2:5 and centrifuged at 4600 *g* for 15 min at 4°C. Subsequently, 300 µL of the aqueous solution was centrifugally filtered through a 5-kDa cut-off filter (Human Metabolome Technologies, Tsuruoka, Japan) to remove proteins. The filtrate was centrifugally concentrated and dissolved in 50 µL of Milli-Q water that contained reference compounds (200 µM each of 3-aminopyrrolidine and trimesate) immediately prior to metabolome analysis.

For palmitate and oleate, after the addition of 400 µL of methanol, pre-weighed, deep-frozen samples (approximately 20 mg each) were completely homogenized using a cell disrupter (Shake Master NEO; Bio Medical Science, Tokyo, Japan) at 1500 rpm for 15 min. The homogenate was then mixed with Milli-Q water and chloroform in a volume ratio of 5:2:5 and centrifuged at 2000 *g* for 5 min at 20°C. Subsequently, 100 µL of the supernatant was used for LC-MS/MS analysis.

Metabolite extraction from HCT116 cells

For metabolite extraction, culture medium and HCT116 cells were collected 48 h after transfection. Then, 100 µL of the collected medium was mixed with 400 µL of methanol containing 25 µM of the internal standards described above, 200 µL of Milli-Q water, and 500 µL of chloroform. The cells were washed twice with ice-cold 5% mannitol solution and covered with 1.2 mL of methanol containing 25 µM internal standards for 10 min. The resulting extracts were mixed with 200 µL of Milli-Q water and 400 µL of chloroform. The aqueous phase of the medium and cell sample solution was then subjected to ultrafiltration as described above.

Metabolome analysis

A critical issue in quantitative analysis using electrospray-based mass spectrometry is the occurrence of matrix effects that may lead to a significant difference in the response of the analytes in the sample compared to a pure standard. To overcome this issue, we used CE-MS for the global analysis of charged metabolites. CE-MS provides high resolution efficiency (theoretical plate numbers greater than 200,000/m), and metabolites are well separated. In addition, unlike LC, charged species are eluted at different migration times based on charge/size ratio in CE. Therefore, most of the charged matrix components are likely separated from analytes in CE-MS. Moreover, the injection volume in CE-MS is quite small (less than 30 nL). Therefore, CE-MS is minimally affected by matrix effects, and this technique provides high quantification accuracy for most analytes in various types of samples.

The concentrations of all the charged metabolites in samples were measured by CE-TOFMS, (Agilent Technologies, Santa Clara, CA) using methods developed by the authors (2, 3). Briefly, to analyze cationic compounds, a fused silica capillary (50 µm i.d. × 100 cm) was used with 1 M formic acid as the electrolyte (4). Methanol/water (50% v/v) containing 0.1 µM hexakis(2,2-difluoroethoxy)phosphazene was delivered as the sheath liquid at 10 µL/min. ESI-TOFMS was performed in positive ion mode, and the capillary voltage was set to 4 kV. Automatic recalibration of each acquired spectrum was achieved using the masses of the reference standards ([^{13}C isotopic ion of a protonated methanol dimer (2 MeOH+H)]$^{+}$, *m*/*z* 66.0632) and ([hexakis(2,2-

difluoroethoxy)phosphazene +H]$^+$, *m/z* 622.0290). To identify metabolites, relative migration times of all peaks were calculated by normalization to the reference compound 3-aminopyrrolidine. The metabolites were identified by comparing their *m/z* values and relative migration times to the metabolite standards. Quantification was performed by comparing peak areas to calibration curves generated using internal standardization techniques with methionine sulfone. The other conditions were identical to those described previously (2).

To analyze anionic metabolites, a commercially available COSMO(+) (chemically coated with cationic polymer) capillary (50 µm i.d. x 105 cm) (Nacalai Tesque, Kyoto, Japan) was used with a 50 mM ammonium acetate solution (pH 8.5) as the electrolyte. Methanol/5 mM ammonium acetate (50% v/v) containing 0.1 µM hexakis(2,2-difluoroethoxy)phosphazene was delivered as the sheath liquid at 10 µL/min. ESI-TOFMS was performed in negative ion mode, and the capillary voltage was set to 3.5 kV. For anion analysis, trimesate and CAS were used as the reference and the internal standards, respectively. The other conditions were identical to those described previously (3).

CE-TOFMS raw data were analyzed using our proprietary software MasterHands (ver, 2.17.0.10). Briefly, the data processing for each experiment included data conversion, binning data into 0.02 *m/z* slices, baseline elimination, peak picking, integration, and elimination of redundant features to yield the all possible peaks lists. Data matrices were generated by an alignment process based on corrected migration times, and metabolite names were assigned to the aligned peaks by matching *m/z* and the corrected migration times of our standards library. Relative peak areas were calculated based on the ratio of peak area divided by those of internal standards, and metabolite concentrations were calculated based on the relative peak area between the sample and standard mixture.

Glucose analysis

LC-MS/MS was performed using an Agilent 1100 series HPLC system (Agilent Technologies) and an Agilent 6430 Triple Quad triple-quadrupole tandem mass spectrometer. The glucose was separated on a TSK-GEL AMIDE-80 column (2 mm i.d. × 250 mm, 5 µm; Tosoh, Tokyo, Japan) that was maintained at 80°C. The mobile phase consisted of water as solution A and acetonitrile as solution B. The elution gradient started with 75% B for 10 min, linearly decreased to 10% B for 2 min and then remained at 10% up to 17 min. The flow rate was 0.2 mL/min, and the injection volume was 0.1 µL. The MS was performed in negative ion mode, and the capillary voltage was set to 4 kV. The flow rate of heated dry nitrogen gas (heater temperature, 300°C) was maintained at 10 L/min. MS/MS with multiple reaction monitoring (MRM) detection was used. At MS/MS, the Q1 (precursor ion), Q3 (product ion), fragmentor and collision energy were set to 179.0 m/z, 89.0 m/z, 60 V and 0 V, respectively. Quantification was performed by comparing the glucose peak area to the calibration curve generated using internal standardization techniques with 2-morpholinoethanesulfonate (MES).

Palmitate and oleate analysis

LC-MS/MS was performed using an Agilent 1290 Infinity HPLC system and an AB Sciex 5500 QTRAP hybrid triple-quadrupole tandem mass spectrometer. Palmitic acid

and oleic acid were separated on an ACQUITY UPLC HSS T3 column (2.1 mm i.d. × 50 mm, 1.8 µm; Waters, Taunton, Ireland) that was maintained at 45°C. The mobile phase consisted of 5 mM ammonium formate aqueous solution containing 1 µM DAEDTA-methanol-acetonitrile (3:1:1, v/v/v) as solution A and isopropanol containing 5 mM ammonium formate and 1 µM DAEDTA as solution B, with a linear gradient from 0 to 40% B for 5 min and from 40 to 64% for 2.5 min, maintenance for 4.5 min, followed by 64 to 82.5% for 0.5 min, from 82.5 to 83.46% for 2.5 min and from 83.46 to 97% for 2.5 min. The flow rate was 0.3 mL/min, and the injection volume was 5 µL. The MS was performed in negative ion mode, and the capillary voltage was set to 4.5 kV. The heated dry nitrogen gas temperature, curtain gas, collision gas and ion source gas were set to 300°C, 30 psi, 6 (arbitrary units) and 50 psi, respectively. MS/MS with multiple reaction monitoring (MRM) detection was used. The declustering potential and collision energy were set to 120 V and 34 V, respectively. The MS/MS transition (Q1/Q3) settings for palmitate and oleate were 256.2/256.2 m/z and 282.2/282.2 m/z, respectively. Quantification was performed by comparing their peak areas to calibration curves generated using internal standardization techniques with reserpine.

Transcriptome analysis

Total RNA was isolated from tissue obtained from 39 colorectal cancer patients (39 normal tissue and 41 tumor tissue samples) using an RNeasy Mini Kit (Qiagen). RNA samples were subjected to expression microarray analysis. The quality of the RNA was assessed using the Agilent 2100 Bioanalyzer (Agilent Technologies). One hundred nanogram aliquots of total RNA were used for the production of Cy3-labeled complementary RNA (cRNA), and all samples were hybridized to the SurePrint G3 Human GE 8x60K v2 microarray (Agilent Technologies). The signal values were extracted using Feature Extraction software (Agilent Technologies). The data for expression microarray analysis were analyzed using GeneSpring software (Agilent Technologies). For microarray analysis of mouse colorectal tissue, wild-type and Apc mutant female mice were euthanized at 14 weeks, and total RNA extracts were used for Cy3-labeled cRNA synthesis. The resulting cRNAs were hybridized to a Mouse GE 4x44K v2 microarray (Agilent Technologies). For analysis of HCT116 cells, total RNA was isolated from cells transfected with control or MYC siRNAs at 48 h post-transfection. The Cy3-labeled cRNAs were hybridized to SurePrint G3 Human GE 8x60K v3 microarray (Agilent Technologies). For normalization of data from human tissue and HCT116 cells, each signal value was divided by the trimmed mean calculated by excluding 2% of the highest and the lowest outliers of all signal values of each sample. For data from mouse tissue, each signal value was divided by the median of all signal values of each sample.

Quantitative real-time PCR analysis

Reverse transcription was performed using ReverTra Ace qPCR RT Master Mix (TOYOBO, Osaka, Japan). Real-time PCR was performed using SYBR Premix Ex Taq II (Tli RNaseH Plus) (Takara Bio, Ohtsu, Japan) and a StepOnePlus Real-Time PCR system (Applied Biosystems, Foster City, CA), following the manufacturer's instructions. Primers were designed using the NCBI Primer-BLAST tool and are listed in table S4.

Targeted sequence
Genomic DNA was extracted from frozen tissue samples with a QIAamp DNA Mini Kit (Qiagen) and then quantified using a Qubit dsDNA BR Assay Kit (Invitrogen) and qPCR (Illumina FFPE QC Kit). Ten nanograms of genomic DNA was used for library construction with the Ion AmpliSeq Cancer Panel v2 (ThermoFisher Scientific, Waltham, MA), which enabled us to examine mutation hotspots in 49 commonly mutated oncogenes and tumor suppressor genes (Fig. S4A). Library DNAs were prepared by amplifying targeted regions by multiplex PCR followed by adapter DNA ligation. The quality of library DNAs was assessed using the Agilent 2100 Bioanalyzer (Agilent Technologies). Emulsion PCR was performed with an Ion OneTouch 200 Template Kit v2 (ThermoFisher Scientific), and sequencing was performed with the Ion PGM System (ThermoFisher Scientific) according to the manufacturer's instructions. We used Torrent Suite software (ThermoFisher Scientific) for automated data analysis. For samples without hotspot mutations in the tumor suppressor genes *APC* or *TP53*, PCR amplification and Sanger sequencing of the PCR products were performed to determine whether other coding regions and splice sites in *APC* or *TP53* contained mutations, according to a previously described protocol (5).

Transmission electron microscopy
Normal and tumor colorectal tissue samples were fixed with 2.5% glutaraldehyde in 0.1 M phosphate buffer (pH 7.4) and then post-fixed with 1% osmium tetroxide in the same buffer. They were dehydrated in a graded series of ethanol and embedded in Epon 812. Ultrathin sections were stained with uranyl acetate and lead citrate and were examined using a JEM-1400 electron microscope (JEOL, Tokyo, Japan).

Immunohistochemistry
Colorectal tissue samples were fixed in formalin, embedded in paraffin wax and sectioned into 4-μm-thick slices. The sections were incubated with mouse monoclonal primary antibodies to TOMM20 (Abcam, Cambridge, United Kingdom, ab56783; 1:100 dilution) and COX IV (Abcam, ab14744; 1:50 dilution), labeled with Histofine Simple Stain MAX PO (MULTI) (Nichirei Biosciences Inc., Tokyo, Japan, code number 424151), and then stained with 3,3'-diaminobenzidine tetrahydrochloride (DAB) solution (Nichirei Biosciences Inc., code number 415171). All sections were counterstained with hematoxylin.

Quantification of mitochondrial DNA content
For quantification of mitochondrial DNA content, the amount of mitochondrial DNA relative to nuclear genomic DNA was determined by qRT-PCR using primers for cytochrome b (a mitochondrial gene) and RPL13A (a nuclear gene), according to a previously described protocol (6).

Methylated DNA immunoprecipitation analysis
Genomic DNA was sonicated to a size range of 100-500 bp. The resulting DNA fragments were ligated to adapters using a standard protocol. Immunoprecipitation of methylated DNA with anti-5-methyl-cytosine antibody was performed using a MagMeDIP kit (Diagenode, Liège, Belgium). Following PCR amplification of

immunoprecipitated DNA, 200-300-bp fragments were size-selected and subjected to 50-bp paired-end sequencing using HiSeq 2000 (Illumina, San Diego, CA). More than 85 million reads (4.2 Gb) were obtained for each sample. The sequencing reads were mapped onto the NCBI build 37.1 (UCSC hg19) assembly of the human genome using the SOAP version 2.20 alignment tool and analyzed with the MACS version 1.4.0 algorithm. The mapped read counts at each locus were normalized with total unique mapped reads in each sample. Data visualization was conducted using GenomeJack (ver. 3.0 Revision 890, Mitsubishi Space Software, Tokyo, Japan).

Software

The data were analyzed with R (ver. 3.2.3, R Foundation for Statistical Computing, Vienna, Austria, www-R-project.org), GraphPad Prism (ver. 5.0.2, GraphPad Software Inc., San Diego, CA), and JMP (ver. 11, SAS, Cary, NC) for statistical analyses; with TM4 software (ver. 4.7.4)[7] for clustering analyses and visualizing the datasets as heat maps; and with XLStat (ver. 2014.1.09, XLStat, Paris, France) and David Bioinformatics Resources (ver. 6.7)[8, 9] for pathway analysis.

Analysis of metabolomics data

For heat map and PCA analyses of human tissue samples, only peaks detected in ≥50% of the subjects in both the tumor and the paired normal tissue were used to eliminate peaks detected in only a few samples. The colors in the heat maps were determined by divided the values by the median values obtained for the normal tissue. For individual metabolites of cultured cells and the medium, the number of molecules in each dish was visualized in bar graphs with the average ± S.D.

To perform PCA in the human tissue samples, mouse samples, and cultured cells, metabolites consistently detected in ≥ 50% of the human tissue and cultured cells (≥ 1) were used. To visualize individual metabolite levels in tumor tissue, box and whiskers plots of metabolites were used. The horizontal bars represent the medians, quartiles, and 10% of both ends. Outliers (≥ average + 3×S.D.) were not visualized, but all data, including outliers, were subjected to statistical analyses. To visualize individual PC levels of the score plots, box and whiskers plots were used, and their horizontal bars indicated medians, quartiles and 5% of both ends. *P*-values were calculated using statistical analyses with two-tailed tests. *P*-values were corrected by false discovery rate (FDR), accommodating multiple independent tests. Error bars at bar graphs indicated the S.D. of the data. To evaluate direct association among human genes, partial correlation were calculated.

To access the correlation between mouse and human metabolomic data, the medians of tumor metabolite concentrations were divided by the medians of control metabolite concentrations, and medians of metabolite concentrations of adenomatous *Apc*$^{+/\Delta 716}$ mouse tissue were divided by the medians of normal metabolite concentrations. The metabolites detected in ≥ 50% of both samples were used and outliers (jackknife α=1.19) were eliminated.

Analysis of gene expression data

To evaluate relative expression levels among multiple genes, each gene was ranked based on the ratio of the median values of tumor and normal samples. To visualize gene

expression levels using box and whiskers plots, each gene expression level was divided by the median value of the control data. The treatment of outliers and horizontal bars was identical to that for the metabolomics data. For the MYC knockdown experiments only, the data were divided by the average of the controls and visualized in a bar graph with means and SDs. *P*-values were corrected by false discovery rate (FDR), accommodating multiple independent tests.

To access the robustness of ranking based on the correlation, we conducted bootstrapping analysis, i.e., the samples were randomly selected, allowing redundant selection to generate datasets with the same sample size, and a statistic test was performed for each dataset. This process was repeated up to 200 times. Finally, 95% confidence intervals were calculated.

To evaluate the correlation between mouse and human transcriptomic data, medians of tumor data were divided by the medians of control data, and medians of adenomatous $Apc^{+/\Delta 716}$ mouse tissue were divided by the medians of normal data. Data with consistent gene symbols between human and mouse tissues, with KEGG E.C. numbers from 1.1 to 1.6, were selected, and outliers (jackknife α=1.18) were eliminated.

SI References

1. Oshima M, et al. (1995) Loss of Apc heterozygosity and abnormal tissue building in nascent intestinal polyps in mice carrying a truncated Apc gene. *Proc Natl Acad Sci USA* 92(10):4482-4486.
2. Soga T, et al. (2006) Differential metabolomics reveals ophthalmic acid as an oxidative stress biomarker indicating hepatic glutathione consumption. *J Biol Chem* 281(24):16768-16776.
3. Soga T, et al. (2009) Metabolomic profiling of anionic metabolites by capillary electrophoresis mass spectrometry. *Anal Chem* 81(15):6165-6174.
4. Soga T & Heiger DN (2000) Amino acid analysis by capillary electrophoresis electrospray ionization mass spectrometry. *Anal Chem* 72(6):1236-1241.
5. Sjoblom T, et al. (2006) The consensus coding sequences of human breast and colorectal cancers. *Science* 314(5797):268-274.
6. Zhang H, et al. (2007) HIF-1 inhibits mitochondrial biogenesis and cellular respiration in VHL-deficient renal cell carcinoma by repression of C-MYC activity. *Cancer Cell* 11(5):407-420.
7. Saeed A, et al. (2003) TM4: a free, open-source system for microarray data management and analysis. *Biotechniques* 34(2):374.
8. Dennis Jr G, et al. (2003) DAVID: database for annotation, visualization, and integrated discovery. *Genome Biol* 4(5):P3.
9. Huang DW, et al. (2007) DAVID Bioinformatics Resources: expanded annotation database and novel algorithms to better extract biology from large gene lists. *Nucleic Acids Research* 35(suppl 2):W169-W175.

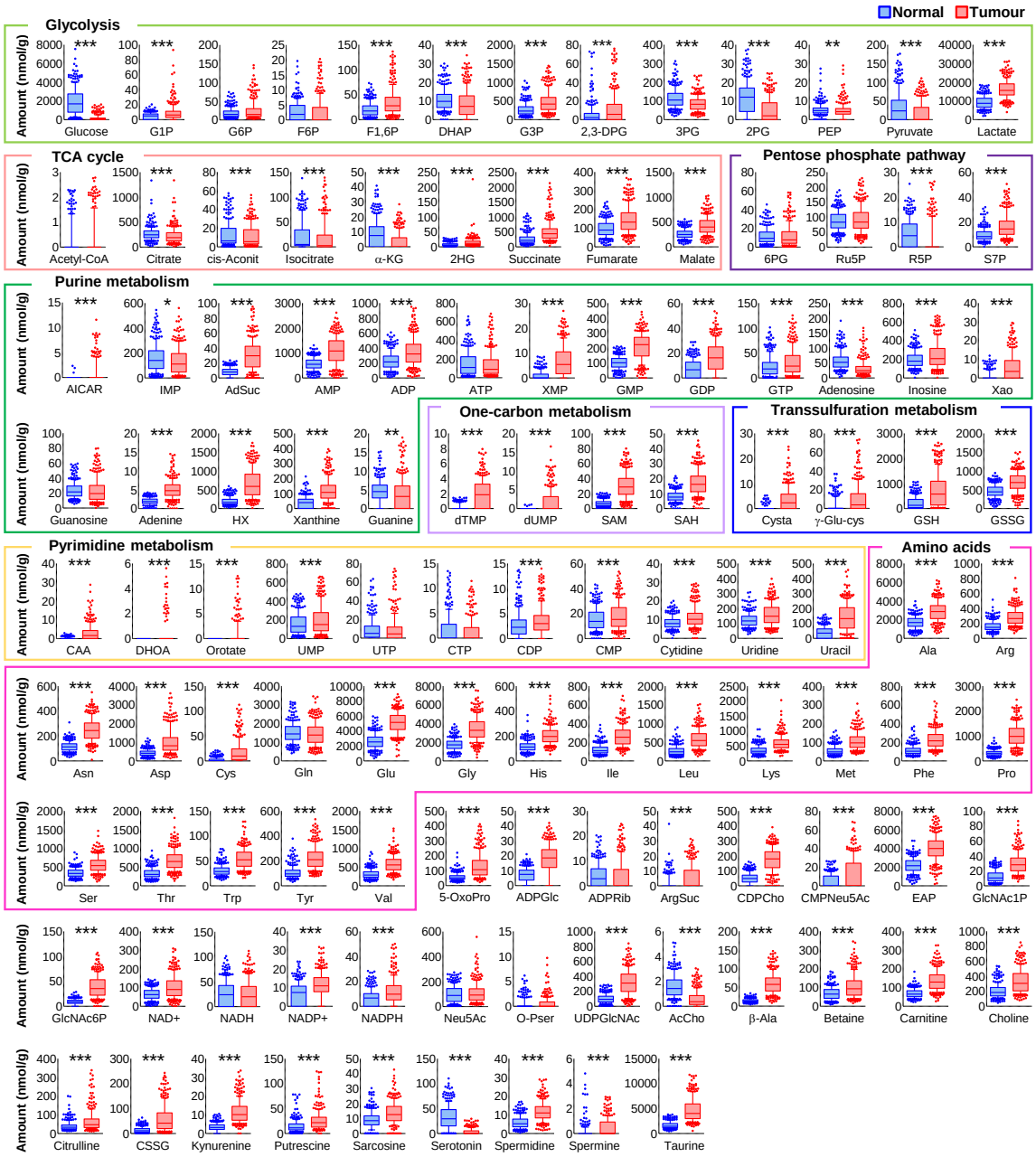

Fig. S1. CE-TOFMS analysis of metabolite levels in paired normal and tumor tissue obtained from 275 CRC patients.

Metabolite abbreviations are listed in Table S2.

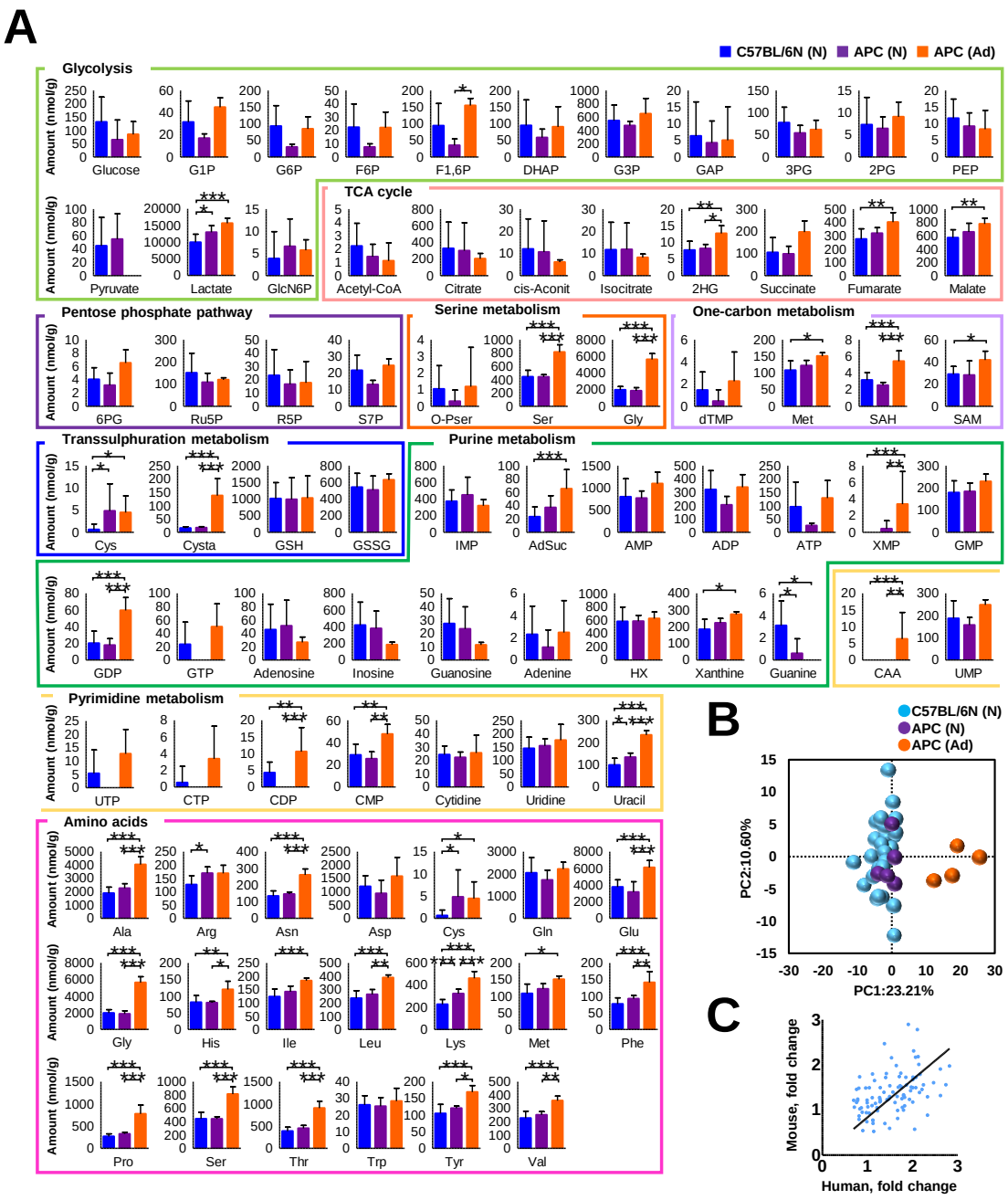

Fig. S2. Metabolite levels change in adenomatous lesions in *Apc* single-mutant mice. **(*A*)** CE-TOFMS analysis of metabolite levels in colorectal normal C57BL/6N mouse tissue (blue, n = 25) and in normal (purple, n = 5) and adenomatous (orange, n = 4) $Apc^{+/\Delta 716}$ mouse tissue. **(*B*)** PCA of colorectal C57BL/6N mouse tissues (blue) and of normal (purple) and adenomatous (orange) $Apc^{+/\Delta 716}$ mouse tissues based on metabolome data. (***C***) Correlation between human and mouse metabolome data. One-way ANOVA and Bonferroni correction were used to determine statistical significance. ***$P < 0.001$, **$P < 0.01$ and *$P < 0.05$. $R = 0.427$ ($P < 0.0001$) for **(*C*)** using Spearman correlation.

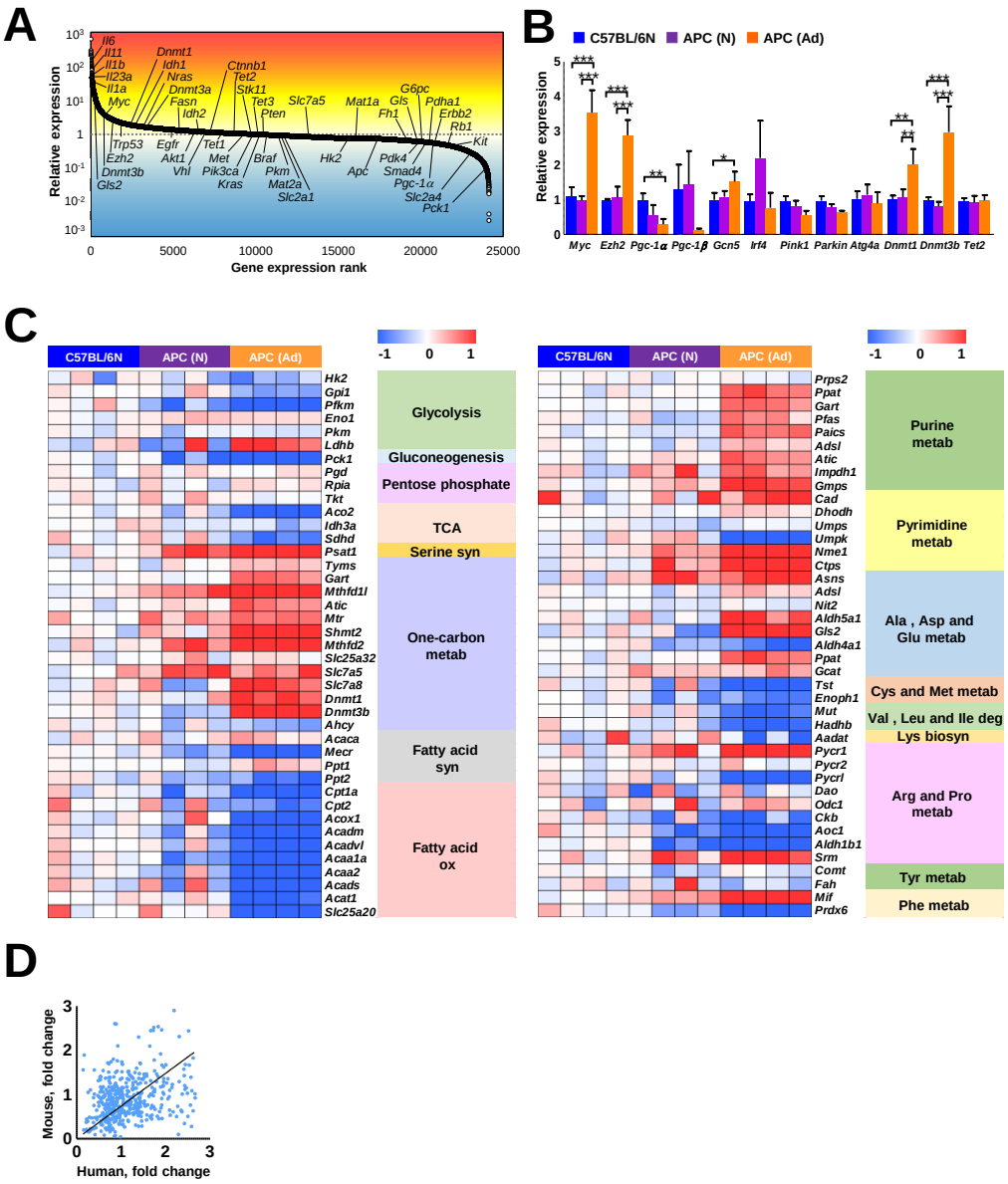

Fig. S3. Gene expression levels change in adenomatous lesions in *Apc* single-mutant mice.

(*A*) Ranking of metabolic genes expressed in $Apc^{+/\Delta 716}$ mouse adenomatous tissue (n = 4) compared with adjacent normal tissue (n = 4). **(*B*)** DNA microarray analysis of genes involved in mitochondrial biogenesis and maintenance and various methylation-promoting genes. **(*C*)** DNA microarray analysis of major metabolic pathway genes in normal C57BL/6N mouse tissue and normal and adenomatous $Apc^{+/\Delta 716}$ mouse tissue. **(*D*)** Correlation between human and mouse transcriptome data. One-way ANOVA and Bonferroni correction were used to determine statistical significance **(*B*)**. ***$P < 0.001$, **$P < 0.01$ and *$P < 0.05$. $R = 0.427$ ($P < 0.0001$) and 0.294 ($P<0.0001$) for **(*D*)** using Spearman correlation.

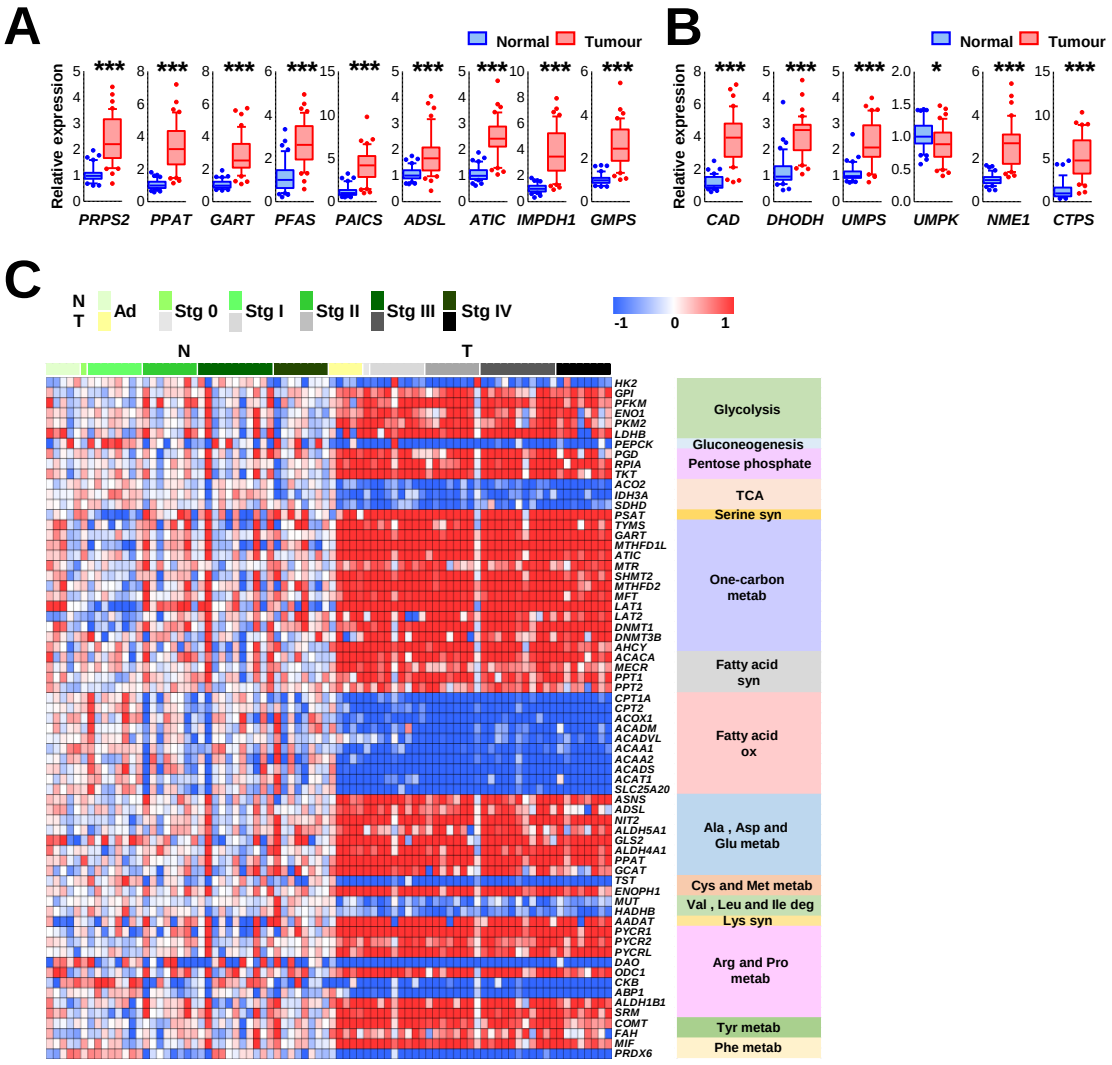

Fig. S4. Expression pattern of many metabolic genes changes along with MYC expression.

(*A*, *B*) DNA microarray analysis of genes involved in *de novo* purine **(*A*)** and pyrimidine **(*B*)** synthesis in normal (blue, n = 39) and tumor (red, n = 41) colorectal tissue. **(*C*)** DNA microarray analysis of major metabolic pathway genes showing correlation coefficients (r^2) greater than 0.4 for *MYC* in normal (n = 39) and tumor colorectal tissue (n = 41). The Wilcoxon signed-rank test was used to determine statistical significance **(*A*, *B*)**. ***$P <$ 0.001 and *$P < 0.05$.

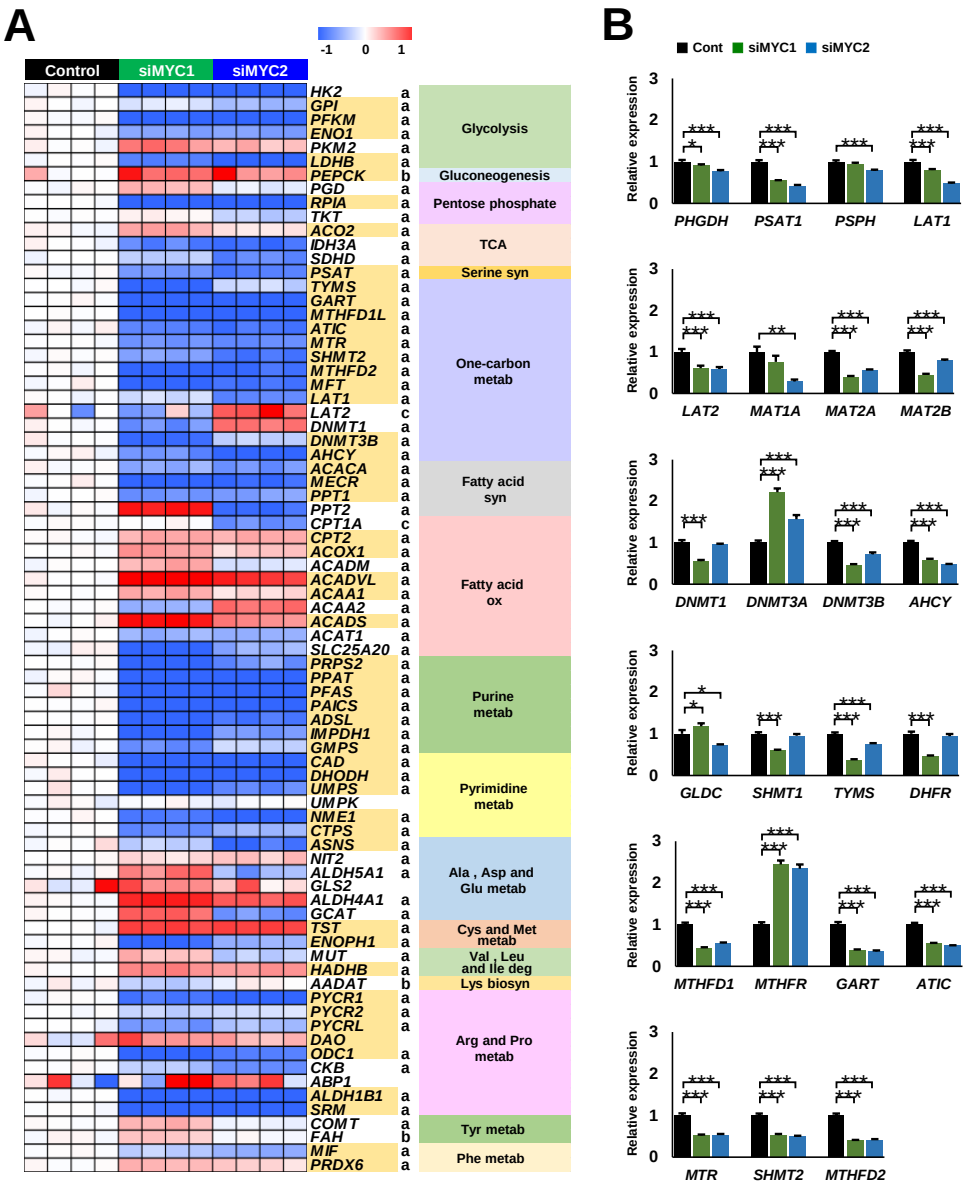

Fig. S5. Knockdown of *MYC* induces changes in the expression pattern of genes related to amino acid- and one-carbon-metabolism in HCT116 cells.

(*A*) DNA microarray analysis of genes related to amino acid metabolism in HCT116 cells transfected with a control siRNA (control) or MYC siRNAs (siMYC1 and siMYC2) (n = 4 each). The genes highlighted in yellow exhibited changes in expression upon MYC knockdown in HCT116 cells that are opposite to those seen in tumor tissues compared with normal tissues in the CRC samples. "a" indicates a significant difference ($P < 0.05$) between the control and both MYC siRNAs. "b" indicates a significant difference ($P < 0.05$) between the control and MYC siRNA1. **(*B*)** qRT-PCR analysis of genes related to serine- and one-carbon-metabolism in HCT116 cells transfected with a control siRNA (Cont) or MYC siRNAs (n = 4 each). Student's *t*-test and Bonferroni correction were used to determine statistical significance. ***$P < 0.001$, **$P < 0.01$ and *$P < 0.05$.

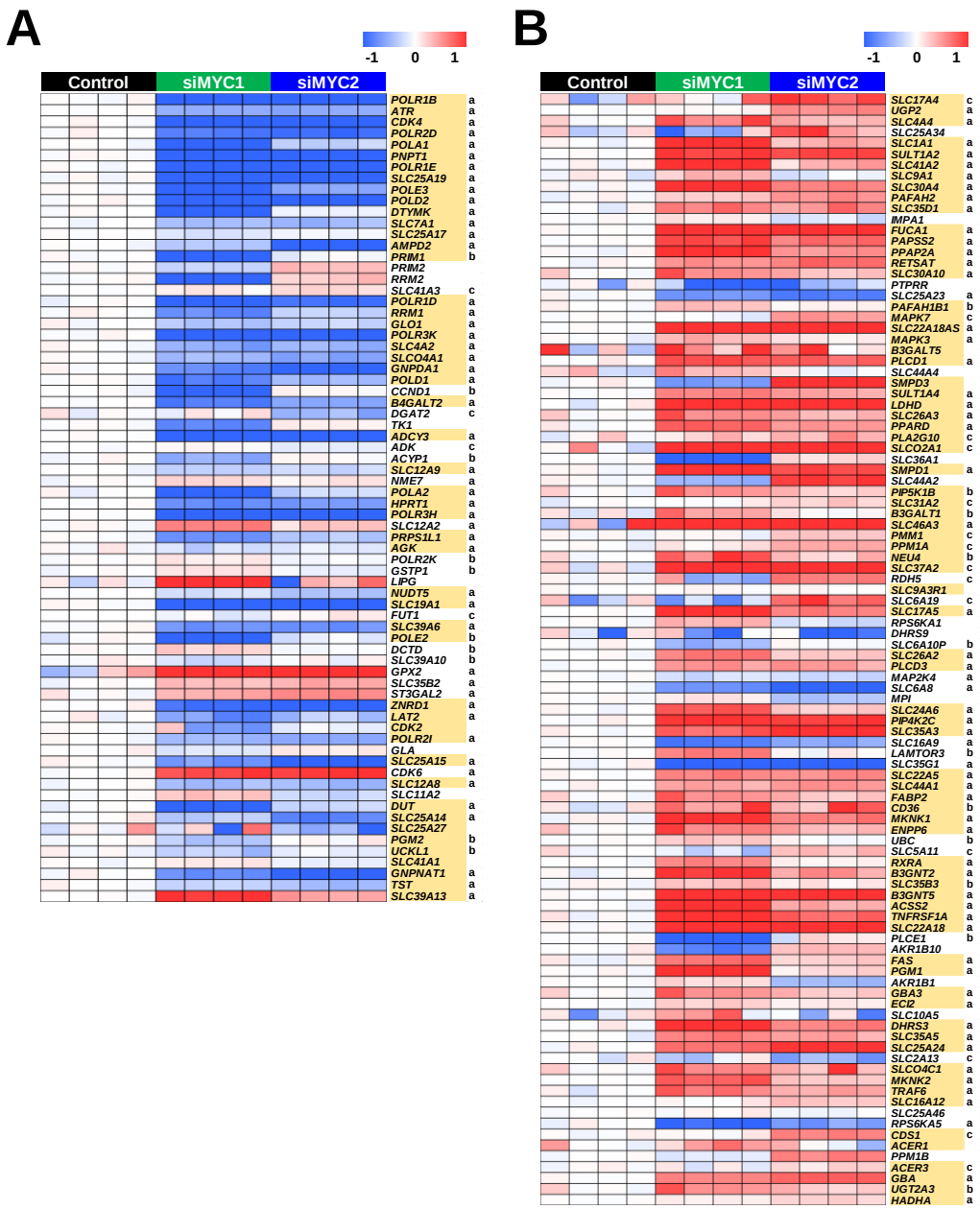

Fig. S6. Knockdown of *MYC* induces changes in the expression pattern of other metabolic genes in HCT116 cells.

(*A*, *B*) DNA microarray analysis of genes in HCT116 cells transfected with control siRNA (control) or MYC siRNAs (siMYC1 and siMYC2) (n = 4 each) that were positively **(*A*)** or inversely **(*B*)** correlated with *MYC* expression in CRC samples (see Fig. 3F and Table S3). The genes highlighted in yellow exhibited changes in expression upon MYC knockdown in HCT116 cells that are opposite to those seen in tumor tissue compared with normal tissue in CRC samples. “a” indicates a significant difference ($P < 0.05$) between the control and both MYC siRNAs. “b” and “c” indicate a significant difference ($P < 0.05$) between control and MYC siRNA1 or MYC siRNA2, respectively. Student’s *t*-test and Bonferroni correction were used to determine statistical significance.

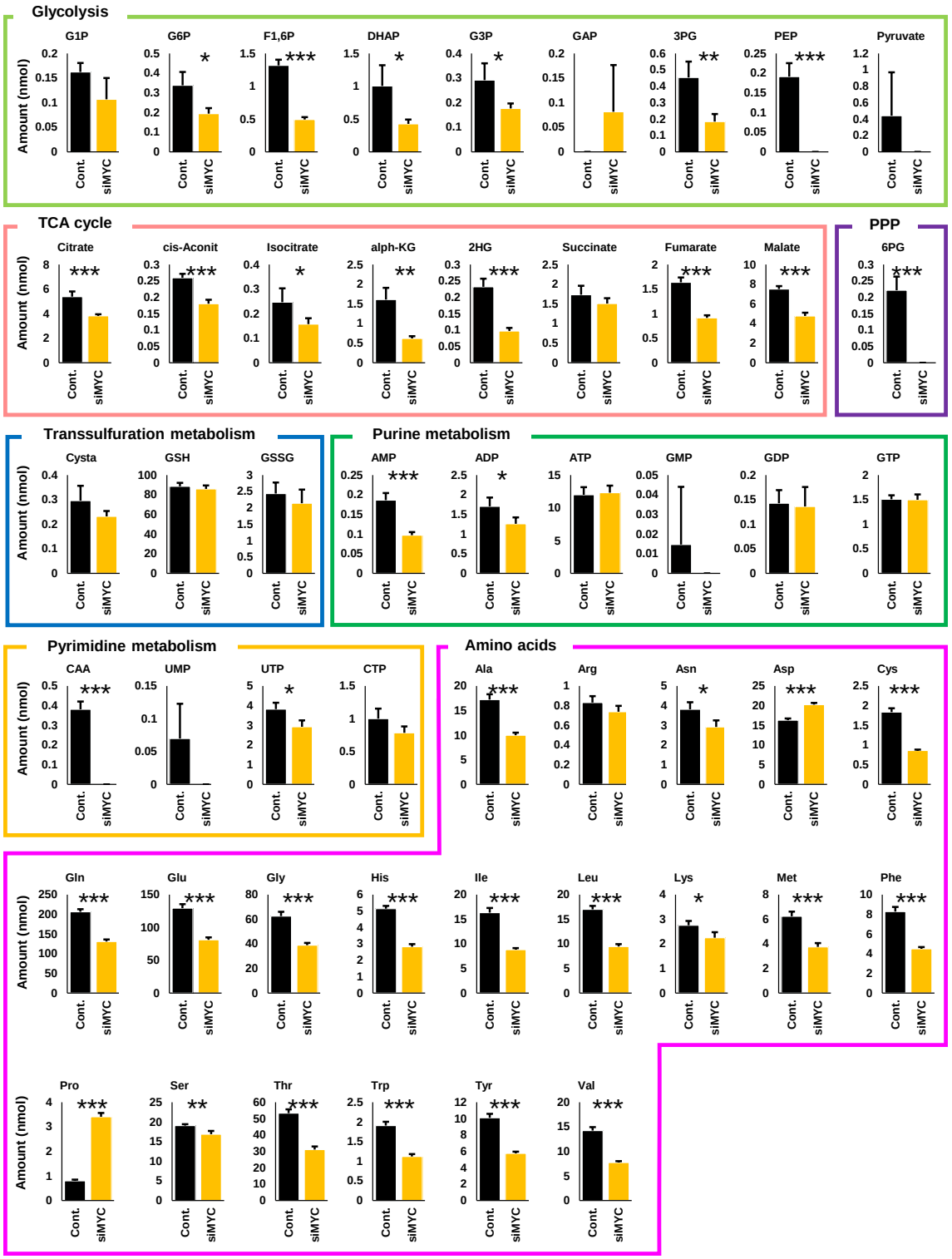

Fig. S7. CE-TOFMS analysis of metabolite amounts in HCT116 cells transfected with a control siRNA or MYC siRNA (n = 4 each).

Student's *t*-test and FDR correlation were used to determine statistical significance. ***P <0.001, **P<0.01, *P<0.05.

Table S1.
Clinicopathological features of patients with colorectal cancer.

UICC Stage	Adenoma	0	I	II	III	IV
Number of cases	5	2	36	102	85	45
Gender						
Male	1	1	22	64	42	25
Female	4	1	14	38	43	20
Age (yrs)						
Median (yr)	77	73	70	73	70	67
Range	52-84	73-74	35-89	35-96	28-92	37-88
Tumor size (mm)						
Median	25	25	27	50	48	52
Min	15	10	10	15	15	12
Max	85	40	63	150	115	160
Tumor location						
Cecum	1	0	2	13	9	4
Appendix	0	0	0	1	1	1
Ascending colon	0	1	6	18	12	6
Transverse colon	1	0	0	6	5	3
Descending colon	0	0	2	8	1	5
Sigmoid colon	1	1	6	20	15	7
Rectum	2	0	20	36	42	17
Not determined	0	0	0	0	0	2
Histology						
Well-differentiated adenocarcinoma	0	2	24	56	35	13
Moderately differentiated adenocarcinoma	0	0	11	33	37	25
Poorly differentiated adenocarcinoma	0	0	0	3	5	2
Mucinous adenocarcinoma	0	0	0	9	5	4
Papillary adenocarcinoma	0	0	1	1	1	1
Signet-ring cell carcinoma	0	0	0	0	1	0
Melanoma	0	0	0	0	1	0

Table S2.

Metabolite abbreviations.

Abbreviation	Compound name	Abbreviation	Compound name
SAM	S-Adenosylmethionine	R5P	Ribose 5-phosphate
SAH	S-Adenosyl-L-homocysteine	S7P	Sedoheptulose 7-phosphate
Glc	Glucose	AICAR	5-Aminoimidazole-4-carboxamide ribonucleotide
O-Pser	O-phosphoserine	AdSuc	Adenylosuccinate
Cysta	Cystathionine	Xao	Xanthosine
γ-Glu-cys	γ-Glutamylcysteine	HX	Hypoxanthine
G1P	Glucose 1-phosphate	CAA	Carbamoylaspartate
G6P	Glucose 6-phosphate	DHOA	Dihydroorotate
F6P	Fructose 6-phosphate	5-OxoPro	5-Oxoproline
F16P	Fructose 1,6-bisphosphate	ADPGlc	ADP-glucose
DHAP	Dihydroxyacetone phosphate	ADPRib	ADP-ribose
G3P	Glycerol 3-phosphate	ArgSuc	Arginosuccinate
2,3-DPG	2,3-Diphosphoglycerate	CDPCho	CDR-choline
3PG	3-Phosphoglycerate	CMPNeu5Ac	CMP-*N*-acetylneuraminate
2PG	2-Phosphoglycerate	EAP	Ethanolamine phosphate
PEP	Phosphoenolpyruvate	GlcNAc1P	*N*-Acetylglucosamine 1-phosphate
cis-Aconit	cis-Aconitate	GlcNAc6P	*N*-Acetylglucosamine 6-phosphate
α-KG	α-Ketoglutarate	Neu5Ac	*N*-Acetylneuraminate
2HG	2-Hydroxyglutarate	UDPGlcNAc	UDP-*N*-acetylglucosamine
6PG	6-Phosphogluconate	AcCho	Acetylcholine
Ru5P	Ribulose 5-phosphate		

Table S3.
Candidate MYC target metabolic genes.

Total of 231 metabolic related genes that showed positively or inversely correlated with MYC expression in CRC tissues (Spearman rank order correlation coefficient: r2 > 0.4).
These are used for Figure 3F. Partial correlations (pr2) of the 231 genes were calculated. All P values of partial correlations were 1.
The genes highlighted in yellow exhibit changes in expression upon MYC knockdown in HCT116 cells that are opposite to those in tumour tissues compared with normal tissues in CRC samples.
*"a" indicates significant differences (P < 0.05) between HCT116 cells transfected with a control siRNA and both MYC siRNAs. "b" and "c" indicate significant differences (P < 0.05) between the control and MYC siRNA1 or MYC siRNA2, respectively.
† "+" indicates genes positively regulated by MYC, whereas "-" indicates inversely regulated.
Genes indicated in black are identified as candidate MYC target genes.

Positively correlated gene	KEGG Pathway	r^2	*P* value	pr^2	*Significance	†Regulation
PAICS	Purine metabolism // Metabolic pathways	0.798	1.43E-29	0.007	a	+
CAD	Pyrimidine metabolism // Alanine, aspartate and glutamate metabolism // Metabolic pathways	0.795	1.79E-29	0.000	a	+
POLR1B	Purine metabolism // Pyrimidine metabolism // Metabolic pathways // RNA polymerase	0.781	8.65E-29	0.013	a	+
ENOPH1	Cysteine and methionine metabolism	0.775	6.00E-28	0.004	a	+
ATR	Fanconi anemia pathway // Cell cycle // p53 signaling pathway // HTLV-I infection	0.773	3.51E-28	0.002	a	+
GART	Purine metabolism // One carbon pool by folate // Metabolic pathways	0.768	1.55E-27	0.033	a	+
CDK4	Cell cycle // p53 signaling pathway // PI3K-Akt signaling pathway // Tight junction // T cell receptor signaling pathway // Hepatitis B // Measles // HTLV-I infection // Pathways in cancer // Viral carcinogenesis // Pancreatic cancer // Glioma // Melanoma // Bladder cancer // Chronic myeloid leukemia // Small cell lung cancer // Non-small cell lung cancer	0.758	7.83E-27	0.118	a	+
GMPS	Purine metabolism // Drug metabolism - other enzymes // Metabolic pathways	0.755	2.25E-26	0.054	a	+
PPAT	Purine metabolism // Alanine, aspartate and glutamate metabolism // Metabolic pathways	0.755	2.85E-26	0.010	a	+
POLR2D	Purine metabolism // Pyrimidine metabolism // Metabolic pathways // RNA polymerase // Huntington's disease // Epstein-Barr virus infection	0.750	8.14E-27	0.035	a	+
POLA1	Purine metabolism // Pyrimidine metabolism // Metabolic pathways // DNA replication	0.747	5.70E-26	0.029	a	+
SLC25A32 (MFT)	Transporter//MFT (mitochondrial folate transporter) One-carbon metabolism	0.744	3.89E-26	0.013	a	+
NME1	Purine metabolism // Pyrimidine metabolism // Metabolic pathways	0.737	1.68E-25	0.013	a	+
POLR1E	Purine metabolism // Pyrimidine metabolism // Metabolic pathways // RNA polymerase	0.735	1.16E-24	0.033	a	+
PNPT1	Purine metabolism // Pyrimidine metabolism // RNA degradation	0.734	7.51E-25	0.018	a	+
DHODH	Pyrimidine metabolism // Metabolic pathways	0.728	1.76E-24	0.007	a	+
MTHFD1L	One carbon pool by folate // Metabolic pathways	0.725	2.76E-24	0.047	a	+
ATIC	Purine metabolism // One carbon pool by folate // Metabolic pathways	0.722	1.52E-24	0.010	a	+
SLC25A19	Transporter	0.719	2.76E-24	0.007	a	+
POLE3	Purine metabolism // Pyrimidine metabolism // Metabolic pathways // DNA replication // Base excision repair // Nucleotide excision repair // HTLV-I infection	0.718	4.59E-24	0.055	a	+
POLD2	Purine metabolism // Pyrimidine metabolism // Metabolic pathways // DNA replication // Base excision repair // Nucleotide excision repair // Mismatch repair // Homologous recombination // HTLV-I infection	0.709	9.53E-24	0.052	a	+
SLC25A17	Transporter	0.708	1.52E-22	0.027	a	+
DTYMK	Pyrimidine metabolism // Metabolic pathways	0.706	1.96E-23	0.011	a	+
SRM	Cysteine and methionine metabolism // Arginine and proline metabolism // beta-Alanine metabolism // Glutathione metabolism // Metabolic pathways	0.703	2.14E-23	0.047	a	+
SLC7A1	Transporter	0.701	3.57E-23	0.018	a	+
CTPS	Pyrimidine metabolism // Metabolic pathways	0.692	1.45E-22	0.023	a	+
PYCR2	Arginine and proline metabolism // Metabolic pathways	0.689	1.26E-22	0.054	a	+
AMPD2	Purine metabolism // Metabolic pathways	0.683	1.81E-22	0.057	a	+
UMPS	Pyrimidine metabolism // Drug metabolism - other enzymes // Metabolic pathways	0.683	6.94E-22	0.143	a	+
PRIM1	Purine metabolism // Pyrimidine metabolism // Metabolic pathways // DNA replication	0.670	8.31E-22	0.001	b	+
PRIM2	Purine metabolism // Pyrimidine metabolism // Metabolic pathways // DNA replication	0.667	1.99E-21	0.012		
RRM2	Purine metabolism // Pyrimidine metabolism // Glutathione metabolism // Metabolic pathways // p53 signaling pathway	0.667	4.43E-21	0.030		
TKT	Pentose phosphate pathway // Metabolic pathways	0.666	3.85E-21	0.087		
PYCR1	Arginine and proline metabolism // Metabolic pathways	0.663	3.06E-21	0.005	a	+
SLC7A5 (LAT1)	Transporter	0.653	1.00E-20	0.103	a	+
AHCY	Cysteine and methionine metabolism // Metabolic pathways	0.642	3.55E-20	0.003	a	+

SHMT2	Glycine, serine and threonine metabolism // Cyanoamino acid metabolism // Glyoxylate and dicarboxylate metabolism // One carbon pool by folate // Metabolic pathways	0.640	1.71E−19	0.021	a	+
PYCRL	Arginine and proline metabolism // Metabolic pathways	0.639	2.58E−19	0.061	a	+
RPIA	Pentose phosphate pathway // Metabolic pathways	0.635	2.25E−19	0.006	a	+
PFAS	Purine metabolism // Metabolic pathways	0.633	1.54E−19	0.082	a	+
IMPDH1	Purine metabolism // Drug metabolism − other enzymes // Metabolic pathways	0.629	2.41E−19	0.005	a	+
RRM1	Purine metabolism // Pyrimidine metabolism // Glutathione metabolism // Metabolic pathways	0.624	1.08E−18	0.002	a	+
SLC41A3	Transporter	0.619	7.25E−19	0.030	c	
POLR1D	Purine metabolism // Pyrimidine metabolism // Metabolic pathways // RNA polymerase // Cytosolic DNA-sensing pathway // Epstein-Barr virus infection	0.618	1.05E−18	0.007	a	+
POLR3K	Purine metabolism // Pyrimidine metabolism // Metabolic pathways // RNA polymerase // Cytosolic DNA-sensing pathway // Epstein-Barr virus infection	0.618	2.56E−18	0.011	a	+
GLO1	Pyruvate metabolism	0.609	2.14E−18	0.079	a	+
SLCO4A1	Transporter	0.605	9.92E−18	0.003	a	+
MTHFD2	One carbon pool by folate // Metabolic pathways	0.600	3.76E−18	0.018	a	+
GPI	Glycolysis / Gluconeogenesis // Pentose phosphate pathway // Starch and sucrose metabolism // Amino sugar and nucleotide sugar metabolism // Metabolic pathways	0.599	1.08E−17	0.030	a	+
ASNS	Alanine, aspartate and glutamate metabolism // Metabolic pathways	0.599	1.04E−17	0.030	a	+
SLC4A2	Transporter	0.599	4.53E−18	0.002	a	+
DGAT2	Glycerolipid metabolism // Metabolic pathways // Fat digestion and absorption	0.596	4.85E−17	0.004	c	
POLD1	Purine metabolism // Pyrimidine metabolism // Metabolic pathways // DNA replication // Base excision repair // Nucleotide excision repair // Mismatch repair // Homologous recombination // HTLV-I infection	0.592	2.29E−17	0.210	a	+
PFKM	Glycolysis / Gluconeogenesis // Pentose phosphate pathway // Fructose and mannose metabolism // Galactose metabolism // Metabolic pathways	0.592	2.82E−17	0.001	a	+
GNPDA1	Amino sugar and nucleotide sugar metabolism // Metabolic pathways	0.591	1.65E−17	0.008	a	+
PRPS2	Pentose phosphate pathway // Purine metabolism // Metabolic pathways	0.588	4.12E−17	0.110	a	+
ODC1	Arginine and proline metabolism // Glutathione metabolism // Metabolic pathways	0.586	3.86E−17	0.054	a	+
TST	Fructose and mannose metabolism // Amino sugar and nucleotide sugar metabolism // Metabolic pathways	0.584	1.46E−10	0.023	a	+
B4GALT2	Galactose metabolism // N-Glycan biosynthesis // Other types of O-glycan biosynthesis // Glycosaminoglycan biosynthesis − keratan sulfate // Glycosphingolipid biosynthesis − lacto and neolacto series // Metabolic pathways	0.583	3.71E−17	0.008	a	+
ALDH4A1	Alanine, aspartate and glutamate metabolism // Arginine and proline metabolism // Metabolic pathways	0.579	1.87E−16	0.011	a	
CCND1	Cell cycle // p53 signaling pathway // PI3K-Akt signaling pathway // Wnt signaling pathway // Focal adhesion // Jak-STAT signaling pathway // Hepatitis B // Measles // HTLV-I infection // Pathways in cancer // Viral carcinogenesis // Colorectal cancer // Pancreatic cancer // Endometrial cancer // Glioma // Prostate cancer // Thyroid cancer // Melanoma // Bladder cancer // Chronic myeloid leukemia // Acute myeloid leukemia // Small cell lung cancer // Non-small cell lung cancer // Viral myocarditis	0.579	3.53E−17	0.011	b	
ADCY3	Purine metabolism // Calcium signaling pathway // Chemokine signaling pathway // Oocyte meiosis // Vascular smooth muscle contraction // Gap junction // Circadian entrainment // Retrograde endocannabinoid signaling // Glutamatergic synapse // Cholinergic synapse // GABAergic synapse // Olfactory transduction // GnRH signaling pathway // Progesterone-mediated oocyte maturation // Melanogenesis // Vasopressin-regulated water reabsorption // Salivary secretion // Gastric acid secretion // Pancreatic secretion // Bile secretion // Morphine addiction // Vibrio cholerae infection // HTLV-I infection // Dilated cardiomyopathy	0.575	1.21E−16	0.031	a	+
POLR3H	Purine metabolism // Pyrimidine metabolism // Metabolic pathways // RNA polymerase // Cytosolic DNA-sensing pathway // Epstein-Barr virus infection	0.575	5.03E−16	0.016	a	+
TK1	Pyrimidine metabolism // Drug metabolism − other enzymes // Metabolic pathways	0.574	1.00E−16	0.027		
ACYP1	Pyruvate metabolism	0.573	3.14E−16	0.029	b	
ADK	Purine metabolism // Metabolic pathways	0.569	2.12E−16	0.000	c	
NME7	Purine metabolism // Pyrimidine metabolism // Metabolic pathways	0.565	3.70E−16	0.013	a	
PRPS1L1	Pentose phosphate pathway // Purine metabolism // Metabolic pathways	0.564	9.38E−16	0.097	a	+
HPRT1	Purine metabolism // Drug metabolism − other enzymes // Metabolic pathways	0.558	4.39E−16	0.001	a	+
PPT1	Fatty acid elongation // Metabolic pathways // Lysosome	0.558	6.06E−16	0.002	a	+
SLC12A2	Transporter	0.556	6.91E−16	0.065	a	
PPT2	Fatty acid elongation // Metabolic pathways // Lysosome	0.556	3.44E−16	0.007		
SLC12A9	Transporter	0.553	3.68E−16	0.014	a	+
AGK	Glycerolipid metabolism // Metabolic pathways	0.549	1.37E−15	0.027	a	+
ADSL	Purine metabolism // Alanine, aspartate and glutamate metabolism // Metabolic pathways	0.546	1.19E−15	0.052	a	+
POLA2	Purine metabolism // Pyrimidine metabolism // Metabolic pathways // DNA replication	0.545	3.96E−16	0.132	a	+

POLR2K	Purine metabolism // Pyrimidine metabolism // Metabolic pathways // RNA polymerase // Cytosolic DNA-sensing pathway // Huntington's disease // Epstein-Barr virus infection	0.533	4.41E-15	0.002	b	
ALDH1B1	Glycolysis / Gluconeogenesis // Pentose and glucuronate interconversions // Ascorbate and aldarate metabolism // Fatty acid metabolism // Valine, leucine and isoleucine degradation // Lysine degradation // Arginine and proline metabolism // Histidine metabolism // Tryptophan metabolism // beta-Alanine metabolism // Glycerolipid metabolism // Pyruvate metabolism // Propanoate metabolism // Metabolic pathways	0.532	3.64E-15	0.002	a	+
SLC19A1	Transporter	0.525	3.12E-14	0.009	a	+
NUDT5	Purine metabolism	0.511	2.90E-14	0.000	a	+
GSTP1	Glutathione metabolism // Metabolism of xenobiotics by cytochrome P450 // Drug metabolism - cytochrome P450 // Pathways in cancer // Chemical carcinogenesis // Prostate cancer	0.507	1.73E-14	0.006	b	
SLC39A6	Transporter	0.506	8.62E-14	0.000	a	+
LIPG	Glycerolipid metabolism // Metabolic pathways	0.505	2.61E-14	0.000		
FUT1	Glycosphingolipid biosynthesis - lacto and neolacto series // Glycosphingolipid biosynthesis - globo series // Metabolic pathways	0.501	6.34E-14	0.001	c	
MECR	Fatty acid elongation // Metabolic pathways	0.499	5.00E-14	0.000	a	+
POLE2	Purine metabolism // Pyrimidine metabolism // Metabolic pathways // DNA replication // Base excision repair // Nucleotide excision repair // HTLV-I infection	0.496	1.21E-13	0.002	b	+
TYMS	Pyrimidine metabolism // One carbon pool by folate // Metabolic pathways	0.496	1.32E-13	0.019	a	+
DCTD	Pyrimidine metabolism // Metabolic pathways	0.491	1.28E-13	0.056	b	
SLC39A10	Transporter	0.489	1.33E-13	0.045	b	
SLC35B2	Transporter	0.487	1.67E-13	0.032	a	
GPX2	Glutathione metabolism // Arachidonic acid metabolism	0.486	1.41E-13	0.008	a	
ZNRD1	Purine metabolism // Pyrimidine metabolism // Metabolic pathways // RNA polymerase	0.479	2.91E-13	0.034	a	+
ST3GAL2	Mucin type O-Glycan biosynthesis // Glycosaminoglycan biosynthesis - keratan sulfate // Glycosphingolipid biosynthesis - globo series // Glycosphingolipid biosynthesis - ganglio series // Metabolic pathways	0.478	1.93E-13	0.010	a	
GLS2	Alanine, aspartate and glutamate metabolism // Arginine and proline metabolism // D-Glutamine and D-glutamate metabolism // Metabolic pathways // Glutamatergic synapse // GABAergic synapse // Proximal tubule bicarbonate reclamation	0.476	4.88E-13	0.073		
GLA	Galactose metabolism // Glycerolipid metabolism // Sphingolipid metabolism // Glycosphingolipid biosynthesis - globo series // Lysosome	0.468	1.36E-12	0.000		
SLC25A15	Transporter	0.464	2.99E-12	0.020	a	+
CDK2	Cell cycle // Oocyte meiosis // p53 signaling pathway // PI3K-Akt signaling pathway // Progesterone-mediated oocyte maturation // Hepatitis B // Measles // Herpes simplex infection // Epstein-Barr virus infection // Pathways in cancer // Viral carcinogenesis // Prostate cancer // Small cell lung cancer	0.462	8.76E-13	0.068		
LDHB	Glycolysis / Gluconeogenesis // Cysteine and methionine metabolism // Pyruvate metabolism // Propanoate metabolism // Metabolic pathways	0.460	3.43E-12	0.028	a	+
SLC7A6 (LAT2)	Transporter	0.459	6.45E-13	0.001	a	+
POLR2I	Purine metabolism // Pyrimidine metabolism // Metabolic pathways // RNA polymerase // Huntington's disease // Epstein-Barr virus infection	0.456	1.10E-12	0.079	a	+
MTR	Cysteine and methionine metabolism // Selenocompound metabolism // One carbon pool by folate // Metabolic pathways	0.456	2.12E-12	0.004	a	+
CDK6	Cell cycle // p53 signaling pathway // PI3K-Akt signaling pathway // Hepatitis B // Measles // Pathways in cancer // Viral carcinogenesis // Pancreatic cancer // Glioma // Melanoma // Chronic myeloid leukemia // Small cell lung cancer // Non-small cell lung cancer	0.452	3.00E-12	0.060	a	
SLC12A8	Transporter	0.448	3.69E-12	0.017	a	+
PKM2	Glycolysis / Gluconeogenesis // Purine metabolism // Pyruvate metabolism // Metabolic pathways // Type II diabetes mellitus // Viral carcinogenesis	0.445	9.10E-12	0.001	a	
SLC25A14	Transporter	0.434	1.34E-11	0.002	a	+
ENO1	Glycolysis / Gluconeogenesis // Metabolic pathways // RNA degradation // HIF-1 signaling pathway	0.432	1.27E-11	0.008	a	+
DUT	Pyrimidine metabolism // Metabolic pathways	0.432	1.12E-11	0.002	a	+
SLC11A2	Transporter	0.432	7.98E-12	0.036		
SLC25A27	Transporter	0.427	1.35E-11	0.000		
PGD	Pentose phosphate pathway // Glutathione metabolism // Metabolic pathways	0.427	1.76E-11	0.037	a	
ALDH5A1	Alanine, aspartate and glutamate metabolism // Butanoate metabolism // Metabolic pathways	0.425	4.96E-11	0.000		
SLC41A1	Transporter	0.419	5.24E-11	0.137		
UCKL1	Pyrimidine metabolism // Drug metabolism - other enzymes // Metabolic pathways	0.419	4.32E-11	0.003	b	+
PGM2	Glycolysis / Gluconeogenesis // Pentose phosphate pathway // Galactose metabolism // Purine metabolism // Starch and sucrose metabolism // Amino sugar and nucleotide sugar metabolism // Metabolic pathways	0.416	2.11E-11	0.005	b	
GNPNAT1	Amino sugar and nucleotide sugar metabolism	0.408	7.08E-11	0.022	a	+

Inversely correlated gene	KEGG Pathway	r^2	*P* value	pr^2	*Significance	†Regulation
SLC17A4	Transporter	0.724	3.88E−25	0.051	c	−
UGP2	Pentose and glucuronate interconversions // Galactose metabolism // Starch and sucrose metabolism // Amino sugar and nucleotide sugar metabolism // Metabolic pathways	0.721	8.62E−24	0.004	a	−
SLC4A4	Transporter	0.697	5.75E−23	0.053	a	−
SULT1A2	Sulfur metabolism // Chemical carcinogenesis	0.667	6.39E−21	0.001	a	−
SLC25A34	Transporter	0.662	2.17E−21	0.081		
SLC9A1	Transporter	0.660	1.88E−20	0.000	a	
SLC1A1	Transporter	0.659	4.83E−21	0.021	a	−
SLC30A4	Transporter	0.658	3.65E−20	0.029	a	−
SLC41A2	Transporter	0.654	1.26E−20	0.144	a	−
SLC35D1	Transporter	0.644	5.27E−20	0.001	a	−
IMPA1	Inositol phosphate metabolism // Metabolic pathways // Phosphatidylinositol signaling system	0.641	7.37E−20	0.106		
PAPSS2	Purine metabolism // Selenocompound metabolism // Sulfur metabolism // Metabolic pathways	0.640	7.80E−20	0.013	a	−
PAFAH2	Ether lipid metabolism // Metabolic pathways	0.639	3.83E−20	0.037	a	−
FUCA1	Other glycan degradation // Lysosome	0.634	7.76E−20	0.002	a	−
PPAP2A	Glycerolipid metabolism // Glycerophospholipid metabolism // Ether lipid metabolism // Sphingolipid metabolism // Metabolic pathways // Fc gamma R−mediated phagocytosis // Fat digestion and absorption	0.631	1.09E−19	0.074	a	−
RETSAT	Retinol metabolism	0.630	1.15E−19	0.041	a	−
PTPRR	MAPK signaling pathway	0.628	4.31E−19	0.033		
MAPK3	MAPK signaling pathway // ErbB signaling pathway // Chemokine signaling pathway // HIF−1 signaling pathway // Oocyte meiosis // mTOR signaling pathway // PI3K−Akt signaling pathway // Vascular smooth muscle contraction // Dorso−ventral axis formation // TGF−beta signaling pathway // Axon guidance // VEGF signaling pathway // Osteoclast differentiation // Focal adhesion // Adherens junction // Gap junction // Toll−like receptor signaling pathway // NOD−like receptor signaling pathway // Natural killer cell mediated cytotoxicity // T cell receptor signaling pathway // B cell receptor signaling pathway // Fc epsilon RI signaling pathway // Fc gamma R−mediated phagocytosis // Circadian entrainment // Long−term potentiation // Neurotrophin signaling pathway // Retrograde endocannabinoid signaling // Glutamatergic synapse // Cholinergic synapse // Serotonergic synapse // Long−term depression // Regulation of actin cytoskeleton // Insulin signaling pathway // GnRH signaling pathway // Progesterone−mediated oocyte maturation // Melanogenesis // Type II diabetes mellitus // Aldosterone−regulated sodium reabsorption // Alzheimer's disease // Prion diseases // Alcoholism // Shigellosis // Salmonella infection // Pertussis // Leishmaniasis // Chagas disease (American trypanosomiasis) // Toxoplasmosis // Tuberculosis // Hepatitis C // Hepatitis B // Influenza A // Pathways in cancer // Viral carcinogenesis // Colorectal cancer // Renal cell carcinoma // Pancreatic cancer // Endometrial cancer // Glioma // Prostate cancer // Thyroid cancer // Melanoma // Bladder cancer // Chronic myeloid leukemia // Acute myeloid leukemia // Non−small cell lung cancer	0.619	1.22E−18	0.000	a	−
SLC25A23	Transporter	0.619	5.49E−19	0.004	a	
SLC30A10	Transporter	0.618	2.41E−19	0.013	a	−
SLC22A18AS	Transporter	0.618	1.19E−18	0.034	a	−
MAPK7	MAPK signaling pathway // Gap junction // Neurotrophin signaling pathway // GnRH signaling pathway	0.616	9.80E−19	0.052	c	
SLC44A4	Transporter	0.616	3.46E−18	0.001		
PAFAH1B1	Ether lipid metabolism	0.611	6.24E−19	0.003	b	−
PLCD1	Inositol phosphate metabolism // Metabolic pathways // Calcium signaling pathway // Phosphatidylinositol signaling system	0.607	3.07E−18	0.000	a	−
B3GALT5	Glycosphingolipid biosynthesis − lacto and neolacto series // Glycosphingolipid biosynthesis − globo series // Metabolic pathways	0.607	1.85E−18	0.002		−
SMPD3	Sphingolipid metabolism // Metabolic pathways	0.601	5.68E−18	0.019		
SLC26A3	Transporter	0.600	1.17E−17	0.014	a	−
LDHD	Pyruvate metabolism	0.600	8.09E−18	0.035	a	−
ACADS	Fatty acid metabolism // Valine, leucine and isoleucine degradation // Butanoate metabolism // Metabolic pathways	0.598	5.50E−18	0.013	a	−
PPARD	PPAR signaling pathway // Wnt signaling pathway // Pathways in cancer // Acute myeloid leukemia	0.598	1.21E−17	0.021	a	−
SULT1A4	Sulfur metabolism // Chemical carcinogenesis	0.595	6.13E−18	0.001	a	−
PLA2G10	Glycerophospholipid metabolism // Ether lipid metabolism // Arachidonic acid metabolism // Linoleic acid metabolism // alpha−Linolenic acid metabolism // Metabolic pathways // Vascular smooth muscle contraction // Pancreatic secretion // Fat digestion and absorption	0.592	1.40E−17	0.001	c	−
SLC36A1	Transporter	0.591	2.58E−17	0.012		
SLCO2A1	Transporter	0.590	1.51E−17	0.000	c	−
SLC44A2	Transporter	0.589	5.95E−17	0.001		
PIP5K1B	Inositol phosphate metabolism // Metabolic pathways // Phosphatidylinositol signaling system // Endocytosis // Fc gamma R−mediated phagocytosis // Regulation of actin cytoskeleton	0.585	1.05E−16	0.001	b	−
PGC1A	Insulin signaling pathway // Adipocytokine signaling pathway // Huntington's disease	0.576	6.75E−17	0.001		
CPT2	Fatty acid metabolism // PPAR signaling pathway	0.574	3.89E−17	0.086	a	−
SMPD1	Sphingolipid metabolism // Metabolic pathways // Lysosome	0.573	5.61E−17	0.074	a	−
PMM1	Fructose and mannose metabolism // Amino sugar and nucleotide sugar metabolism // Metabolic pathways	0.572	3.31E−16	0.036	c	−

ACAA1	Fatty acid metabolism // Valine, leucine and isoleucine degradation // alpha-Linolenic acid metabolism // Biosynthesis of unsaturated fatty acids // Metabolic pathways // PPAR signaling pathway // Peroxisome	0.569	2.80E-16	0.002	a	-
MUT	Valine, leucine and isoleucine degradation // Glyoxylate and dicarboxylate metabolism // Propanoate metabolism // Metabolic pathways	0.567	4.58E-16	0.000		
B3GALT1	Glycosphingolipid biosynthesis - lacto and neolacto series // Metabolic pathways	0.565	1.60E-16	0.011	b	-
SLC46A3	Transporter	0.565	2.87E-16	0.068	a	-
SLC31A2	Transporter	0.562	1.25E-16	0.003	c	-
RDH5	Retinol metabolism	0.557	1.07E-15	0.026	c	
SLC37A2	Transporter	0.556	1.04E-15	0.005	c	-
SLC6A19	Transporter	0.556	1.16E-15	0.009	c	
ACAA2	Fatty acid elongation // Fatty acid metabolism // Valine, leucine and isoleucine degradation // Metabolic pathways	0.554	6.30E-16	0.013		
PPM1A	MAPK signaling pathway	0.553	3.92E-16	0.011	c	-
RPS6KA1	MAPK signaling pathway // Oocyte meiosis // mTOR signaling pathway // Long-term potentiation // Neurotrophin signaling pathway // Progesterone-mediated oocyte maturation	0.546	1.70E-15	0.001		
NEU4	Other glycan degradation // Sphingolipid metabolism	0.545	8.31E-16	0.075	b	-
SLC9A3R1	Transporter	0.545	1.12E-15	0.005		
SLC25A20	Transporter	0.542	6.19E-16	0.015	a	
SLC26A2	Transporter	0.537	3.48E-15	0.040	a	-
DHRS9	Retinol metabolism // Metabolic pathways	0.536	2.75E-15	0.004		
SLC17A5	Transporter	0.533	1.17E-15	0.000	a	-
PLCD3	Inositol phosphate metabolism // Metabolic pathways // Calcium signaling pathway // Phosphatidylinositol signaling system	0.532	3.98E-15	0.001	a	-
CPT1A	Fatty acid metabolism // PPAR signaling pathway // Adipocytokine signaling pathway	0.528	8.03E-15	0.019	c	
MAP2K4	MAPK signaling pathway // ErbB signaling pathway // Toll-like receptor signaling pathway // Fc epsilon RI signaling pathway // GnRH signaling pathway // Epithelial cell signaling in Helicobacter pylori infection // Chagas disease (American trypanosomiasis) // Hepatitis B // Influenza A // HTLV-I infection // Epstein-Barr virus infection	0.527	7.72E-15	0.002	a	
ACO2	Citrate cycle (TCA cycle) // Lysine biosynthesis // Glyoxylate and dicarboxylate metabolism // Metabolic pathways // 2-Oxocarboxylic acid metabolism	0.526	4.58E-15	0.025	a	-
SLC6A8	Transporter	0.521	1.24E-14	0.005	a	
SLC6A10P	Transporter	0.521	2.83E-15	0.003	b	
SLC24A6	Transporter	0.518	1.48E-14	0.004	a	-
LAMTOR3	MAPK signaling pathway	0.512	3.44E-14	0.000	b	
SLC35G1	Transporter	0.512	4.33E-14	0.110	a	
MPI	Fructose and mannose metabolism // Amino sugar and nucleotide sugar metabolism // Metabolic pathways	0.508	1.37E-14	0.000		
SLC16A9	Transporter	0.506	3.30E-14	0.081	a	
PIP4K2C	Inositol phosphate metabolism // Phosphatidylinositol signaling system // Regulation of actin cytoskeleton	0.505	3.03E-14	0.005	a	-
SLC35A3	Transporter	0.501	3.30E-14	0.005	a	-
CD36	PPAR signaling pathway // Phagosome // ECM-receptor interaction // Hematopoietic cell lineage // Adipocytokine signaling pathway // Fat digestion and absorption // Malaria	0.500	1.20E-13	0.002	b	-
SLC22A5	Transporter	0.496	4.89E-14	0.017	a	-
MKNK1	MAPK signaling pathway // HIF-1 signaling pathway // Insulin signaling pathway	0.492	1.51E-13	0.003	a	-
SLC44A1	Transporter	0.490	1.04E-13	0.062	a	-
SDHD	Citrate cycle (TCA cycle) // Oxidative phosphorylation // Metabolic pathways // Alzheimer's disease // Parkinson's disease // Huntington's disease	0.488	1.45E-13	0.000	a	
FABP2	PPAR signaling pathway // Fat digestion and absorption	0.485	1.14E-13	0.003	a	-
ENPP6	Ether lipid metabolism	0.484	1.63E-13	0.000	a	-
RXRA	PPAR signaling pathway // Adipocytokine signaling pathway // Bile secretion // Hepatitis C // Pathways in cancer // Transcriptional misregulation in cancer // Thyroid cancer // Small cell lung cancer // Non-small cell lung cancer	0.483	3.90E-13	0.112	a	-
SLC5A11	Transporter	0.479	3.09E-13	0.072	c	
ACADM	Fatty acid metabolism // Valine, leucine and isoleucine degradation // beta-Alanine metabolism // Propanoate metabolism // Metabolic pathways // PPAR signaling pathway	0.478	3.14E-13	0.047		
B3GNT5	Glycosphingolipid biosynthesis - lacto and neolacto series // Metabolic pathways	0.478	6.45E-13	0.057	a	-
SLC35B3	Transporter	0.471	5.64E-13	0.036	b	-
ACSS2	Glycolysis / Gluconeogenesis // Pyruvate metabolism // Propanoate metabolism // Metabolic pathways	0.470	8.26E-13	0.002	a	-
B3GNT2	Glycosaminoglycan biosynthesis - keratan sulfate // Glycosphingolipid biosynthesis - lacto and neolacto series // Metabolic pathways	0.470	4.37E-13	0.003	a	-
SLC22A18	Transporter	0.469	1.17E-12	0.019	a	-
PLCE1	Inositol phosphate metabolism // Metabolic pathways // Calcium signaling pathway // Phosphatidylinositol signaling system	0.469	1.26E-12	0.002	b	
TNFRSF1A	MAPK signaling pathway // Cytokine-cytokine receptor interaction // NF-kappa B signaling pathway // Apoptosis // Osteoclast differentiation // Adipocytokine signaling pathway // Alzheimer's disease // Amyotrophic lateral sclerosis (ALS) // Chagas disease (American trypanosomiasis) // Toxoplasmosis // Tuberculosis // Hepatitis C // Influenza A // HTLV-I infection // Herpes simplex infection	0.468	9.03E-13	0.001	a	-
UBC	PPAR signaling pathway	0.467	3.06E-13	0.000	b	

IDH3A	Citrate cycle (TCA cycle) // Metabolic pathways // 2-Oxocarboxylic acid metabolism	0.464	8.21E-13	0.020	a	
AKR1B10	Pentose and glucuronate interconversions // Fructose and mannose metabolism // Galactose metabolism // Glycerolipid metabolism // Pyruvate metabolism // Metabolic pathways	0.460	1.31E-12	0.159		
PEPCK	Glycolysis / Gluconeogenesis // Citrate cycle (TCA cycle) // Pyruvate metabolism // Metabolic pathways // PPAR signaling pathway // PI3K-Akt signaling pathway // Insulin signaling pathway // Adipocytokine signaling pathway // Proximal tubule bicarbonate reclamation	0.457	1.76E-12	0.003	b	-
PGM1	Glycolysis / Gluconeogenesis // Pentose phosphate pathway // Galactose metabolism // Purine metabolism // Starch and sucrose metabolism // Amino sugar and nucleotide sugar metabolism // Metabolic pathways	0.457	2.66E-12	0.003	a	-
SLC10A5	Transporter	0.453	9.39E-12	0.011		
FAS	MAPK signaling pathway // Cytokine-cytokine receptor interaction // p53 signaling pathway // Apoptosis // Natural killer cell mediated cytotoxicity // Type I diabetes mellitus // Alzheimer's disease // Chagas disease (American trypanosomiasis) // African trypanosomiasis // Hepatitis B // Measles // Influenza A // Herpes simplex infection // Pathways in cancer // Autoimmune thyroid disease // Allograft rejection // Graft-versus-host disease	0.449	2.49E-12	0.002	a	-
AKR1B1	Pentose and glucuronate interconversions // Fructose and mannose metabolism // Galactose metabolism // Glycerolipid metabolism // Pyruvate metabolism // Metabolic pathways	0.446	4.54E-12	0.161		
GBA3	Cyanoamino acid metabolism // Starch and sucrose metabolism // Metabolic pathways	0.443	6.15E-12	0.001	a	-
SLC35A5	Transporter	0.442	1.29E-11	0.043	a	-
SLC25A24	Transporter	0.440	1.32E-11	0.003	a	-
ECI2	Fatty acid metabolism // Peroxisome	0.436	8.12E-12	0.030	a	-
HK2	Glycolysis / Gluconeogenesis // Fructose and mannose metabolism // Galactose metabolism // Starch and sucrose metabolism // Amino sugar and nucleotide sugar metabolism // Butirosin and neomycin biosynthesis // Metabolic pathways // HIF-1 signaling pathway // Insulin signaling pathway // Type II diabetes mellitus // Carbohydrate digestion and absorption	0.428	1.77E-11	0.005	a	
DHRS3	Retinol metabolism // Metabolic pathways	0.425	1.20E-11	0.002	a	-
TRAF6	MAPK signaling pathway // NF-kappa B signaling pathway // Ubiquitin mediated proteolysis // Endocytosis // Osteoclast differentiation // Toll-like receptor signaling pathway // NOD-like receptor signaling pathway // RIG-I-like receptor signaling pathway // Neurotrophin signaling pathway // Pertussis // Leishmaniasis // Chagas disease (American trypanosomiasis) // Toxoplasmosis // Tuberculosis // Hepatitis C // Measles // Herpes simplex infection // Epstein-Barr virus infection // Pathways in cancer // Small cell lung cancer	0.423	3.87E-11	0.009	a	-
SLC2A13	Transporter	0.421	1.84E-11	0.000	c	
SLC16A12	Transporter	0.420	4.02E-11	0.000	a	-
HADHB	Fatty acid elongation // Fatty acid metabolism // Valine, leucine and isoleucine degradation // Metabolic pathways	0.419	3.07E-11	0.001	a	-
MKNK2	MAPK signaling pathway // HIF-1 signaling pathway // Insulin signaling pathway	0.414	3.04E-11	0.008	a	-
SLC25A46	Transporter	0.413	5.25E-11	0.002		
ACAT1	Fatty acid metabolism // Synthesis and degradation of ketone bodies // Valine, leucine and isoleucine degradation // Lysine degradation // Tryptophan metabolism // Pyruvate metabolism // Glyoxylate and dicarboxylate metabolism // Propanoate metabolism // Butanoate metabolism // Terpenoid backbone biosynthesis // Metabolic pathways	0.412	5.96E-11	0.085	a	
SLCO4C1	Transporter	0.411	2.17E-11	0.056	a	-
CDS1	Glycerophospholipid metabolism // Metabolic pathways // Phosphatidylinositol signaling system	0.410	7.41E-11	0.133	c	-
ACER3	Sphingolipid metabolism	0.408	1.19E-10	0.033	c	
ACER1	Sphingolipid metabolism // Metabolic pathways	0.407	7.99E-11	0.001		
PPM1B	MAPK signaling pathway	0.406	8.77E-11	0.110		
RPS6KA5	MAPK signaling pathway // Circadian entrainment // Neurotrophin signaling pathway // Bladder cancer	0.405	6.35E-11	0.042	a	
UGT2A3	Pentose and glucuronate interconversions // Ascorbate and aldarate metabolism // Steroid hormone biosynthesis // Starch and sucrose metabolism // Retinol metabolism // Porphyrin and chlorophyll metabolism // Metabolism of xenobiotics by cytochrome P450 // Drug metabolism - cytochrome P450 // Drug metabolism - other enzymes // Metabolic pathways // Chemical carcinogenesis	0.400	1.26E-10	0.055	b	-

Table S4.
Oligonucleotide sequences.

siRNA oligonucleotides	
MYC siRNA1 (siMYC1)	5′-GCUUGUACCUGCAGGAUCU-3′
MYC siRNA2 (siMYC2)	5′-CGAUGUUGUUUCUGUGGAA-3′
MYC siRNA3 (siMYC3)	5′-CGUCCAAGCAGAGGAGCAA-3′
CAD siRNA1 (siCAD1)	5′-GAGUAUGAGGGUCUCUUCU-3′
CAD siRNA2 (siCAD2)	5′-GGAUCAAAGCCAUUGUGCA-3′
UMPS siRNA1 (siUMPS1)	5′-CCAAUCAAAUUCCAAUGCU-3′
UMPS siRNA2 (siUMPS2)	5′-GAGUUGAUAACUCUGGCAA-3′
CTPS siRNA1 (siCTPS1)	5′-CCAUGUUGAGCCUGAACAA-3′
CTPS siRNA2 (siCTPS2)	5′-GAAACUCUAUGGAGACGCA-3′
TYMS siRNA1 (siTYMS1)	5′-CAAUGGAUCCCGAGACUUU-3′
TYMS siRNA2 (siTYMS2)	5′-GGAAUCAGAUUAUUCAGGA-3′
PPAT siRNA1 (siPPAT1)	5′-GAAAUGGUCUGGAAUGUUU-3′
PPAT siRNA2 (siPPAT2)	5′-GAAAAGAGUGGUCAUUGUA-3′
GART siRNA1 (siGART1)	5′-GGAAUAAUGCUGACCAAGA-3′
GART siRNA2 (siGART2)	5′-CAAAUACCGCCAUCUCAAU-3′
ATIC siRNA1 (siATIC1)	5′-GUUGCAUUGUCCGAUGUUU-3′
ATIC siRNA2 (siATIC2)	5′-CAGAGAAGUAUCUGAUGGU-3′
PGC-1α siRNA1 (siPGC-1α-1)	5′-CAGUGAUUUCAGUAAUGAA-3′
PGC-1α siRNA2 (siPGC-1α-2)	5′-CUGAAGUCCUCUUGCAAGA-3′
PGC-1β siRNA1 (siPGC-1β-1)	5′-CAGAUACACUGACUACGAU-3′
PGC-1β siRNA2 (siPGC-1β-2)	5′-CAAGCAUAGUCUAGGCAAA-3′
Control siRNA pool	5′-UGGUUUACAUGUCGACUAA-3′
	5′-UGGUUUACAUGUUGUGUGA-3′
	5′-UGGUUUACAUGUUUUCUGA-3′
	5′-UGGUUUACAUGUUUUCCUA-3′
Quantitative real-time PCR primers	
β-actin-forward	5′-CCAGCCTTCCTTCCTGGGCATGG-3′
β-actin-reverse	5′-TTGGCGTACAGGTCTTTGCGGAT-3′
MYC-forward	5′-CCACCAGCAGCGACTCTGAGGAG-3′
MYC-reverse	5′-TGCCAGGAGCCTGCCTCTTTTCC-3′
CAD-forward	5′-TGGGAGCTGCATGAAGAGCGTTG-3′
CAD-reverse	5′-TCCTCAAATGAACGCCCAATGCC-3′
EZH2-forward	5′-TGTGGACCACAGTGTTACCAGCA-3′
EZH2-reverse	5′-GTGAGAGCAGCAGCAAACTCCTT-3′
GCN5-forward	5′-TGCTGTCACCTCGAATGAGCAGG-3′
GCN5-reverse	5′-CAGGTGGTTCATCAGGTGGGTCC-3′

PINK1-forward	5′-GGCCGGACGCTGTTCCTCGTTAT-3′
PINK1-reverse	5′-TTCACACAAAGGTACTGGCGCA-3′
Parkin-forward	5′-CAGGAAGGACTCACCACCAGC-3′
Parkin-reverse	5′-GACAGGGGCCTTTGCAATACACAT-3′
PHGDH-forward	5′-AGAGGAGCTGATAGCGGAGCTG-3′
PHGDH-reverse	5′-CCTTGGTGGCAGAGCGAACAATA-3′
PSAT1-forward	5′-AGCTCCTTGTACAACACGCCTCC-3′
PSAT1-reverse	5′-CACTCCAGAACCAAGCCCATGAC-3′
PSPH-forward	5′-GGTGCCACAGATATGGAAGCCTGT-3′
PSPH-reverse	5′-GTTGCCTGATCACATTTCCTCCA-3′
LAT1-forward	5′-CACAGAAAGCCTGAGCTTGAGCG-3′
LAT1-reverse	5′-GAGGCAGGCCAGGATGAAGAACA-3′
LAT2-forward	5′-AGATAGTCCTTCGCTGGAAGAAGC-3′
LAT2-reverse	5′-ATGATGGGGAACAGCAGGTTGAT-3′
MAT1A-forward	5′-AGCCCAGTGGGCGGTTTGTCATC-3′
MAT1A-reverse	5′-TAATCTTACGGCCAGTGACACCC-3′
MAT2A-forward	5′-TCCTTTTCACCTCAGAGTCGGTCG-3′
MAT2A-reverse	5′-GGACAGCATCACTGATTTGGTCACA-3′
MAT2B-forward	5′-ATTAGATGGAGAAAAGGCTGTCCTG-3′
MAT2B-reverse	5′-ATAGGAATCCTCAAAACAGCAGC-3′
DNMT1-forward	5′-CGCGAGATTCGAGTCCCCTCCA-3′
DNMT1-reverse	5′-ACGGGCACAGCTCACACAGAAT-3′
DNMT3A-forward	5′-CTACTTCTGGGGTAACCTTCCCG-3′
DNMT3A-reverse	5′-ATCATTCACAGTGGATGCCAACG-3′
DNMT3B-forward	5′-CCAGGACTCGTTCAGAAAGCCCA-3′
DNMT3B-reverse	5′-TCCCGGCTGGAGACACTGTTGTT-3′
AHCY-forward	5′-GGAGAAGGTGAACATCAAGCCGC-3′
AHCY-reverse	5′-GCGGCGCCCATTCTTCAACCGAT-3′
GLDC-forward	5′-TTTGCGGAACTTACTGGAGAACTCA-3′
GLDC-reverse	5′-CCCTGAGACACCTCAGGCTGGTA-3′
SHMT1-forward	5′-CTGCCGAGCTGGCATGATCTTCT-3′
SHMT1-reverse	5′-TTGCCAGTCTTGGGATCCACACTT-3′
TYMS-forward	5′-TGTTTTGGAGGAGTTGCTGTGGTT-3′
TYMS-reverse	5′-CACTCCCTTGGAAGACAGCTCTTTA-3′
DHFR-forward	5′-GAATGACCACAACCTCTTCAGTAGAA-3′
DHFR-reverse	5′-GAATGGAGAACCAGGTCTTCTTACC-3′
MTHFD1-forward	5′-CCAGCAGCTTCCAGCTCCTTTATG-3′
MTHFD1-reverse	5′-TAGATCTTCTGTGCAATGATCCTGA-3′
MTHFR-forward	5′-TCTTCCCTCCTCGAACTGCTGAG-3′
MTHFR-reverse	5′-ACCTGCTGCCATCCGGTCAAAC-3′
GART-forward	5′-CTTTCACCAAACCTGAAGAAGCCT-3′

GART-reverse	5′-ACTGGCCTTCACAACCAAAGCAG-3′
ATIC-forward	5′-GCAAAAGCTCTCAGGGATGCTGG-3′
ATIC-reverse	5′-AAATCCCGTCAACTCAGAGACATC-3′
MTR-forward	5′-GCGCTCCAAGACCTGTCGCAACC-3′
MTR-reverse	5′-GATCTCATCCCGCAGGGTTTTCT-3′
SHMT2-forward	5′-GACTTCCGAGTTGCGATGCTGTA-3′
SHMT2-reverse	5′-TGACCAGCTGCCCACATCTCTG-3′
MTHFD2-forward	5′-ACGATCCTGTAACTGCCAAACCCA-3′
MTHFD2-reverse	5′-TATACCCAGCTTTTTGTCTGACTC-3′
PAICS-forward	5′-TGGGGAGTTCAGGATGTGTGGTCT-3′
PAICS-reverse	5′-AAAGTACGGTTGAACAGCCAAGA-3′
MTHFD1L-forward	5′-AGGCGCTGGGTTCATTTACCCTT-3′
MTHFD1L-reverse	5′-GCAGTCCTGGCATGGTGCTCAT-3′
CTPS-forward	5′-TCTCAAGAAACGTGCTGGGATGG-3′
CTPS-reverse	5′-GACCACGGGATGACTGGTCGTAG-3′
UMPS-forward	5′-CTGGCCACTGGGGACTACACTAGA-3′
UMPS-reverse	5′-TCAGAGTGCTCCTCAGCCATTCT-3′
PPAT- forward	5′-AATGGCGAATTGGTAAATGCTGCT-3′
PPAT- reverse	5′-TAGACAGACCAATACCATGACGCA-3′
PYCR1-forward	5′-AGGCCTCCTGCATCCGCACAC-3′
PYCR1-reverse	5′-CGGCTGGTGACACCTGCTCCTG-3′
PGC-1α-forward	5′-CCACACACAGTCGCAGTCACAAC-3′
PGC-1α-reverse	5′-TTGGTGACTCTGGGGTCAGAGGA-3′
PGC-1β-forward	5′-TCACCAGCCACTCGAAGGAACTT-3′
PGC-1β-reverse	5′-CGGATGCTTGGCGTTCTGTCTGA-3′
Cytochrome b-forward	5′-GCGTCCTTGCCCTATTACTATC-3′
Cytochrome b-reverse	5′-ATATGGAGGATGGGGATTATTGCT-3′
RPL13A-forward	5′-GCCCTGGAATGTACGGGACCCAG-3′
RPL13A-reverse	5′-CCAGCTTCCTATGTCCCAGGGC-3′